Journal of Chromatography A, 1217 (2010) 928–940

Contents lists available at ScienceDirect

Journal of Chromatography A

journal homepage: www.elsevier.com/locate/chroma

Review

Nuclear magnetic resonance approaches to the rationalization of chromatographic enantiorecognition processes

Gloria Uccello-Barretta*, Letizia Vanni, Federica Balzano

Università degli Studi di Pisa, Dipartimento di Chimica e Chimica Industriale, Via Risorgimento 35, I-56126 Pisa, Italy

ARTICLE INFO

Article history:
Available online 1 November 2009

Dedicated to Prof. Volker Schurig, Tübingen, on the occasion of his 70th birthday.

Keywords:
Reviews
Nuclear magnetic resonance
Chromatography
Chiral recognition
Chiral separation
Mechanisms

ABSTRACT

NMR spectroscopy represents a valuable tool for obtaining information about structure and dynamics at a molecular level on the diastereoisomeric complexes formed by enantiomeric substrates and chromatographic chiral selectors or modifiers. Some examples collected from the literature show the potentialities of solution NMR spectroscopy in the rationalization of chromatographic enantiorecognition processes and the different NMR approaches needed according to the chiral selector features.

Contents

1. Introduction

The considerable importance of chiral separation of drugs, pharmaceuticals and agrochemicals implies the need for the development of rapid, reproducible and efficient chromatographic methods. Knowledge of chiral recognition mechanisms opens new perspectives on the rational design of chiral selectors endowed with widespread applicability. Understanding of the interaction mechanisms, which are often the basis of enantiorecognition processes, relies on the exploitation of the considerable potentialities of spectroscopic methods, above all, nuclear magnetic resonance (NMR). Spontaneous assembly of molecules into non-covalently bound structured aggregates represents the basis of molecular recognition on which separation sciences rely and an understanding of molecular recognition phenomena involves analysis of different aspects of architecture and organization assembly processes.

Various chiral selectors have been used in enantioselective chromatography, such as polysaccharides, cyclodextrins, proteins, Pirkle's types selectors, alkaloids, macrocyclic antibiotics and crown ethers. Polymers imprinted with chiral templates represent tailor-made stationary phases with predictable selectivity.

Chiral selectors provide a diastereoisomeric environment for the enantiomers with formation of transient complexes, which are stabilized by a number of interactions, such as hydrogen bonds, π–π, dipole–dipole, ionic and steric interactions. Diastereoiso-

* Corresponding author. Tel.: +390502219232; fax: +390502219260.
E-mail address: gub@dcci.unipi.it (G. Uccello-Barretta).

0021-9673/$ – see front matter © 2009 Elsevier B.V. All rights reserved.
doi:10.1016/j.chroma.2009.10.070

meric derivatives of the enantiomeric substrates having different physicochemical properties are formed in the stationary phases or in the mobile phase, and are therefore separated.

NMR spectroscopy is applicable to all the most important aspects of molecular recognition phenomena. Resonances of the single different nuclei which are present in the molecular systems under investigation can be detected and several NMR parameters are correlated to structural features by means of a large number of NMR pulse sequences, which are in continuous evolution, also by virtue of the widespread availability of highly sophisticated high-field NMR spectrometers. As a matter of fact, since Pirkle's pioneering work in 1986 [1], the last 20 years have witnessed an intense synergy between NMR and chromatographic methods.

Here a general survey of NMR investigations of chromatographic enantioselective molecular recognition processes will be presented, without claiming to give an exhaustive and complete analysis of the data in the literature. Even though there are numerous valuable papers on this topic, only those examples will be selected that are relevant from a historical point of view or that highlight the ability of NMR spectroscopic techniques to satisfy the investigation needs of chiral selectors with very different structural features.

2. NMR methods

Primarily, NMR value relies on the opportunities it offers for the investigation of recognition phenomena at a molecular level by determination of: (a) stereochemistry and dynamics of supramolecular complexes, also including macromolecular systems; (b) evaluation of their thermodynamic parameters. The stereochemistry and dynamics of assembled species can be investigated using NOE or ROE methods [2]. The dependence of NMR parameters on concentration or temperature gradients, assisted by suitable data analysis methods, can be exploited for the analysis of thermodynamic parameters [3,4]. DOSY diffusion NMR methods [5–7] of measurement of translational diffusion coefficients D can be applied to the monitoring of assembly at the oligomer level, complementary to light-scattering techniques for larger size particles in solution or transmission electron microscopy in the solid state, by virtue of D dependence on hydrodynamic radius (R_H). Diffusion methods are very effective in the analysis of complexation phenomena that lead to a remarkable increase of apparent sizes of complexing species.

Anisochrony of corresponding nuclei of enantiomeric mixtures is the manifestation of chiral recognition phenomena in NMR spectra, which is due to the ability of selected chiral auxiliaries to generate their detectable diastereoisomeric derivatives.

In solutions containing mixtures of the selected enantiomerically pure chiral auxiliary (**A**) and enantiomeric mixtures of the chiral substrate (**B**), two complexation equilibria must be considered in which each enantiomer is present as a free and bound species:

$$\boldsymbol{A} + (S)\text{-}\boldsymbol{B} \rightleftarrows (S)\text{-}\boldsymbol{B}\cdot\boldsymbol{A} \quad \text{and} \quad \boldsymbol{A} + (R)\text{-}\boldsymbol{B} \rightleftarrows (R)\text{-}\boldsymbol{B}\cdot\boldsymbol{A}$$

In the fast-exchange conditions, which are frequently fulfilled, only one signal is observed for the bound and free forms of each enantiomer and the observed NMR parameter (P^R_{obs}, P^S_{obs}), Eq. (1), is the molar fraction weighted average of the same parameters in the free ($P^R_f = P^S_f$) and bound (P^R_b, P^S_b) forms

$$P^R_{obs} = X^R_f P^R_f + X^R_b P^R_b \quad \text{and} \quad P^S_{obs} = X^S_f P^S_f + X^S_b P^S_b \tag{1}$$

where X_f and X_b are the molar fractions of the free and bound species, respectively.

Possibility to devise interaction models relies on the availability of several local parameters, such as chemical shifts, coupling constants and relaxation rates that assume different values for the different nuclei inside the molecule and are highly responsive to local effects produced by selector–selectand interactions. Investigations of thermodynamic features of diastereoisomeric solvates not only rely on the dependence of the above-mentioned local parameters on concentration or selector–selectand molar ratios, but also on the opportunity offered by NMR spectroscopy to detect rotational or translational motions by determining diffusion coefficients or reorientational correlation times, which assume only one value (isotropic motions) for the whole molecule and, hence, are particularly responsive to the slowing-down of molecular motions due to complexation phenomena.

Analysis of complexation parameters [3] of the two diastereoisomeric solvates should include analysis of the self-aggregation propensity of both chiral auxiliaries and enantiomeric substrates, which is fundamental in selecting the optimal experimental conditions for the analysis of heterocomplexation phenomena. The presence of self-association phenomena is clearly evaluated by analysing the NMR spectra of the pure component in progressively diluted solutions: when chemical shifts depend on the concentration, the self-association constant should be determined. To this end, in more simple and common self-aggregation, i.e. dimerization, we combine Eq. (2), which defines the measured chemical shift (δ_{obs}) as the weighted average of its value in the monomer (δ_m) and dimer (δ_d), with that of dimerization constant, Eq. (3), in order to obtain the dependence of observed chemical shifts on the initial concentration C_0.

$$\delta_{obs} = X_m\delta_m + X_d\delta_d \tag{2}$$

$$K_d = \frac{X_d}{2C_0(1-X_d)^2} \tag{3}$$

The dimerization constant can be determined by non-linear fittings of experimental dilution data on the basis of suitable equations (Eqs. (4)–(6) are examples) describing such a dependence [8–10].

$$\Delta_{obs} = \frac{4K_dC_0 + 1 - \sqrt{1+8K_dC_0}}{4K_dC_0}\Delta_d - \Delta_r \tag{4}$$

where $\Delta_{obs} = \delta_r - \delta_{obs}$, $\Delta_d = \delta_m - \delta_d$, $\Delta_r = \delta_m - \delta_r$ and δ_r is the chemical shift of a reference compound;

$$\delta_{obs} = \delta_m + (\delta_d - \delta_m)\frac{\sqrt{1+8K_dC_0}-1}{\sqrt{1+8K_dC_0}+1} \tag{5}$$

and

$$C_0 = \frac{(\delta_{obs}-\delta_m)(\delta_d-\delta_m)}{2K_d(\delta_d-\delta_{obs})^2} \tag{6}$$

Alternatively, diffusion coefficients, strongly sensitive to aggregation phenomena, could reveal the real nature of the self-associated forms.

The dependence of diffusion coefficients on molecular sizes is given by the Stokes–Einstein equation, Eq. (7), which strictly holds only for spherical molecules

$$D = \frac{kT}{c\pi\eta R_H} \tag{7}$$

where R_H is the hydrodynamics radius, k the Boltzmann constant, T the absolute temperature, η the solution viscosity and c a numerical factor, which is assumed to be equal to 6 when solvent radius is significantly smaller than molecule radius; alternatively it can be suitably corrected by exploiting semi-empirical approaches [11,12]. Solution viscosity is usually considered approximately equal to solvent viscosity, even though use an internal standard is recommended [13] to correct viscosity changes caused by solute presence. Suitable viscosity standards are spherical molecules

which do not interact with molecules under investigation. For molecules that deviate from sphericity, shape models [14,15] can be employed, but this topic is of interest only in cases in which Eq. (7) is employed to extract distance values and this case is not often met with in investigations regarding chiral recognition phenomena.

The most important aspect of diffusion detection by NMR is that diffusion coefficients are affected by molecular sizes and they become a direct proof of aggregation phenomena. When aggregation occurs, we would expect an increase of molecular radius which, in the fast-exchange conditions, depends on the degree of self-aggregation (association constant) as well as on the nature of self-associated forms. At the concentrations that are commonly employed in NMR investigations, self-assembly to a dimer level can be assumed to be the most favourable process.

In the analysis of the heterocomplexation phenomena involved in the formation of the two diastereoisomers, the heterocomplexation parameters to be determined are complexation stoichiometries and association constants and, in principle, any NMR parameter can be employed, but usually chemical shift determinations are preferred, even though recently the use of diffusion coefficients, obtained by NMR DOSY techniques [3,16], are gaining in popularity in the determination of association constants.

In the cases of low dimerization constants, the self-association processes can be neglected, otherwise self-aggregation phenomena must be taken into consideration, analysing the presence of simultaneous equilibria or selecting experimental conditions for analysis for which self-association phenomena are discouraged (as in low concentrations of the dimerizing species in the presence of high molar excesses of the complexing agent). As far as the heterocomplexation parameters are concerned, stoichiometry is usually determined from NMR data by means of Job's method [17], analysing the chemical shifts of solutions with different molar ratios of the two components **A** and **B**, but with constant total concentrations. The data are plotted in the form $X_B \Delta\delta^B$ ($\Delta\delta^B = \delta^B_{obs} - \delta^B_f$) versus X_A. The abscissa of the maximum is correlated to the stoichiometry of the complex. Alternatively, in the presence of strong complexes ($K > 10^5$) the mole ratio method, involving the preparation of a series of solutions containing constant concentration of **B** and a suitable range of concentration of **A**, works well [3]. Two straight lines, intersecting at the [**A**]/[**B**] ratio corresponding to the stoichiometry of complexation, are obtained by plotting $\Delta\delta^B$ against [**A**].

Once the stoichiometry of complexation has been determined, separate NMR experiments must be carried out to measure the heteroassociation constants of the two diastereoisomeric complexes. Two different experimental conditions can be considered: a constant low concentration of one component in the presence of increasing excesses of the other or equimolar mixtures progressively diluted. In both cases, the equation giving the measured chemical shift (δ_{obs}) as the weighted average of the chemical shifts of the uncomplexed (δ_f) and complexed (δ_b) species is combined with the equation giving the association constant on the basis of the complex stoichiometry.

In this way, the dependence of the experimental observations (chemical shifts) on the initial concentrations is obtained in a form that is suitable for linear fittings (Eqs. (8)–(10)) [18–20]

$$\frac{1}{\Delta\delta} = \frac{1}{K\Delta\delta_{max}[B_0]} + \frac{1}{\Delta\delta_{max}} \tag{8}$$

where $\Delta\delta = \delta_{obs} - \delta_f$, $\Delta\delta_{max} = \delta_b - \delta_f$, $[B_0]$ is the concentration of the component in large excess;

$$\frac{\Delta\delta}{[B_0]} = -K\Delta\delta + K\Delta\delta_{max} \tag{9}$$

$$\frac{[B_0]}{\Delta\delta} = \frac{[B_0]}{\Delta\delta_{max}} + \frac{1}{K\Delta\delta_{max}} \tag{10}$$

or non-linear fitting methods [3]. The latter do not require approximations and large excesses of one species are not mandatory. Moreover, they allow for the processing of stoichiometries different from 1:1. However, they require the development of suitable computer programs for treatment of NMR data [3].

Titrations are no longer required when the heteroassociation involves small molecules interacting with large molecules as in the cases of host–guest complexes [3]. Indeed, the diffusion of small molecules is mainly controlled by the diffusion of large molecules and, hence, the diffusion parameter of small molecules in the bound state (D_b) can be approximated as the diffusion coefficient of the large complexing agent.

On the above hypothesis, D_b parameter of Eq. (11) (holding in the fast-exchange conditions) is not an unknown parameter

$$D_{obs} = X_f D_f + X_b D_b \tag{11}$$

Taking into consideration that D_f is the diffusion coefficient of the pure compound, the molar fraction of the bound species X_b, expressed by Eq. (12), and, therefore, heteroassociation constant, can be determined by single point experiments.

$$X_b = \frac{D_{obs} - D_f}{D_b - D_f} \tag{12}$$

It should be remarked that this kind of approximated approach could give rise to significant errors when association constants are very low or very high. In the first case the D_{obs} parameter is very similar to the D_f one, in the latter one the D_{obs} value is very similar to the D_b parameter. Thus it has been suggested [21] that both chemical shifts and diffusion parameters be used in titration experiments within the appropriate range of complexation degrees (20–80%) as a prerequisite to obtaining accurate results. Also a factor which must be considered is the superior sensitivity of chemical shift determinations.

Knowledge of the association constants of the two diastereoisomeric complexes is essential for determining their relative stabilities and for evaluating the suitable concentration to be used in the NMR conformational investigations in order to analyse solutions containing detectable amounts of complexed species (at least 30%). The possibility of evaluating by NMR association constants of diastereoisomeric solvates directly in the mixtures containing racemate, instead of pure enantiomers, is very attractive from the practical point of view [22,23].

To ascertain conformational aspects, preliminary information regarding the intermolecular interactions can be obtained directly from the analysis of the ^{1}H NMR spectra in terms of the complexation shifts ($\Delta\delta = \delta_{obs} - \delta_f$) measured for all the nuclei of the two species. However, the most important method of conformational analysis in the definition of the binding geometry is the detection of dipolar interactions (NOEs) [2], which reflect the spatial proximity between nuclei and, therefore, highlight proximity constraints between nuclei located inside the same molecule (intramolecular dipolar interactions) or belonging to different molecules (intermolecular dipolar interactions). Intramolecular dipolar interactions allow the definition of the conformation of the chiral auxiliary or enantiomeric substrates both in the free state and in the diastereoisomeric complexes and, therefore, the identification of the nature of conformational changes due to complexation, if occurring. Intermolecular dipolar interactions make it possible to define the relative stereochemistry of the chiral auxiliary and one or other of the enantiomers in the two diastereoisomeric complexes.

Dipolar interactions can be detected by using mono- and bidimensional NOESY and ROESY techniques [2]. The intensities of NOEs can be correlated to the interproton distances r_{ij} between protons *ij*.

A quick method for obtaining the interproton distances are proton mono- (R_i) and biselective (R_{ij}) relaxation rates measurements

[24], respectively obtained by inverting the magnetization of one proton *i*, or simultaneously spin *i* and the spin *j*, and following the recovery to the equilibrium of the magnetization of *i*. The difference between the biselective and monoselective relaxation rates gives the cross-relaxation parameter σ_{ij} of the proton pair *ij*,

$$\sigma_{ij} = R_{ij} - R_i \tag{13}$$

which, in the initial rate approximation [25], is a simple function of the reorientational correlation time τ_c of the vector connecting the two protons and of their interproton distance r_{ij} as expressed by Eq. (14):

$$\sigma_{ij} = 0.1\gamma^4\hbar^2 r_{ij}^{-6}\tau_c \left[\frac{6}{1+4\omega^2\tau_c^2} - 1\right] \tag{14}$$

where γ is the proton gyromagnetic ratio, ω is the proton Larmor frequency and $\hbar$ is the reduced Planck's constant. In the fast motion regime ($\omega^2\tau_c{}^2 \ll 1$) the above equation becomes:

$$\sigma_{ij} = 0.5\gamma^4\hbar^2 r_{ij}^{-6}\tau_c \tag{15}$$

In the slow motion region ($\omega^2\tau_c{}^2 \gg 1$) Eq. (14) assumes the approximated form of Eq. (16):

$$\sigma_{ij} = -0.1\gamma^4\hbar^2 r_{ij}^{-6}\tau_c \tag{16}$$

On the hypothesis of isotropic molecular motion, the ratios between the cross-relaxation parameters of two proton pairs depend on the inverse ratios of the sixth powers of their interproton distances:

$$\frac{\sigma_{ij}}{\sigma_{ik}} = \frac{r_{ik}^6}{r_{ij}^6} \tag{17}$$

Therefore, when in the molecule there is a proton pair having a fixed and known distance, we can calculate any other distance in the molecule and, therefore, define its conformation.

It is noteworthy that cross-relaxation parameters (Eqs. (15)–(17)), which are commonly determined also by 1D and 2D NOE methods, are very sensitive to the motion regime of molecules. Hence, they can be used as a proof of the dynamic changes produced by aggregation phenomena.

Other geometrical parameters, such as dihedral angles, can also be determined by analysing the dependence of vicinal coupling constants on the dihedral angles on the basis of empirical relationships (Karplus, Altona) [26,27].

3. Small sized chiral selectors

Papers published by Pirkle in 1986–1987 [1,28] are milestones in the field of chromatographic enantiorecognition rationales, which were supported by spectroscopic investigations in solution. The basic idea of his work was to investigate by NMR the stereochemistry and the thermodynamic features of diastereoisomeric solvates which were formed by a suitable soluble model of the chromatographic selector and the two enantiomers of a chiral analyte which was efficiently enantiodiscriminated on the corresponding chiral stationary phase (CSP). In spite of the fact that at that time NMR spectrometers and methods were not as advanced as at present, the authors examined thoroughly all those aspects that are relevant to the investigation of chiral recognition processes involving small sized chiral selectors.

Very detailed direct spectroscopic investigations regarding the interaction between chiral analytes and CSPs are made difficult by the presence of the solid support. However, on the hypothesis that interactions at the achiral solid support do not affect interaction mechanisms significantly and that linkages to silica do not cause significant conformational changes, diastereoisomeric solvates formed in solution between soluble analogues of CSPs and analyte enantiomers could be used as models for chromatographic enantiorecognition. Pirkle reported the efficient enantiodiscrimination of *N*-(2-naphthyl)alanine esters on a CSP derived from (*S*)-*N*-(3,5-dinitrobenzoyl)leucine, as well as enantiomeric amides of *N*-(3,5-dinitrobenzoyl)leucine were well separated on the CSP derived from *N*-(2-naphthyl)alanine [1,29]. Since in the first case separations were only marginally affected by changes in the length of the ester alkoxy moiety of the analyte, it was concluded that enantiorecognition did not depend to any great extent on the nature or proximity of the solid support. Thus the interaction between (*S*)-*N*-(3,5-dinitrobenzoyl)leucine *n*-propylamide (**1**) and the two enantiomers of *N*-(2-naphthyl)alanine methyl ester (**2**) (Fig. 1) was investigated by NMR in $CDCl_3$ as solvent to support a chiral recognition model. The two solutions containing S(analyte)–S(selector) and R(analyte)–S(selector) were also different in colour.

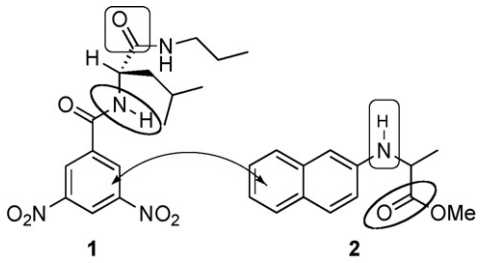

Fig. 1. Structures of analyte and CSP soluble model, **1** and **2**, with indication of the three simultaneous attractive interactions occurring in the (S)-**1**/(S)-**2** diastereoisomer.

Some inconsistencies in the values of association constants obtained by NMR titration methods involving the use of the chiral selector at low or high concentration suggested possible occurrence of self-aggregation processes of the chiral selector to a dimer level or even higher level aggregates. In fact, dilution experiments indicated the dependence of proton chemical shifts of pure selector on concentration gradients, which was fitted on the basis of a suitable equation to give $K_{dimer} = 50 \pm 10\ M^{-1}$. Stereochemistry of the dimer was assumed to be head-to-tail dimer, which was also confirmed on the basis of selected NOE effects. Drastic changes in chemical shifts in S–S mixtures demonstrated that dimerization was inhibited by heteroassociation, whereas it remained the favoured association mechanism for the other pair.

In order to determine the true K_{ass} for the (*S*,*S*)-complex, high analyte/selector ratios were employed, which discouraged self-association of the selector. Values obtained by ^1H NMR titrations were in good agreement with UV data. Analysis of temperature dependence of association constants led the authors to calculate the value for ΔH of −4.75 kcal/mol, which was quite in agreement with the formation of two hydrogen bonds selector-(*S*)-analyte and a π−π attractive interaction. Also longitudinal relaxation times of (*S*)-analyte underwent significant decreases due to the increased reorientational time consequent to the formation of the complex. Interestingly some protons showed T_1s variations which were indicative of conformational changes due to complexation phenomena.

Most of the intermolecular NOEs in the (*S*,*S*)-complex were observed for the aryl protons of the selector and (S)-analyte, only a single dipolar intermolecular interaction was detected in the other pair. On the basis of proximity constraints imposed by NOE effects together with the analysis of complexation shifts, an interaction model for the (*S*)-**1**/(*S*)-**2** diastereoisomer was constructed, which was in agreement with the previously reported interaction mechanism obtained on the basis of chromatographic data. In this model (Fig. 1) (*S*)-**1**/(*S*)-**2** diastereoisomer is stabilized by three attractive interactions: a π−π interaction between the two aromatic moi-

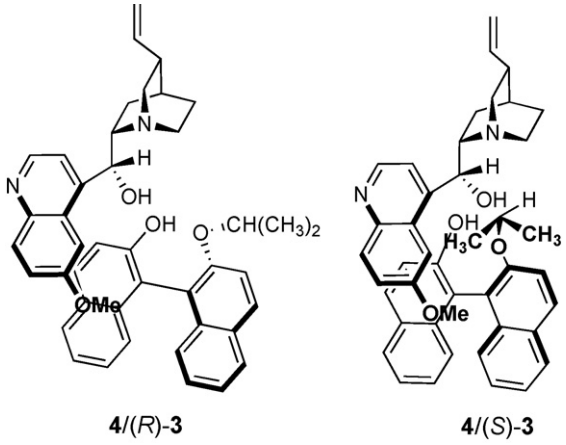

Fig. 2. Graphical representation of interaction mechanisms in the (*R*)-**3**/**4** and (*S*)-**3**/**4** diastereoisomers.

eties of (*S*)-**1** and (*S*)-**2** and one hydrogen bond between the amide proton of (*S*)-**1** and the carbonyl oxygen of (*S*)-**2**, which cooperate with the attractive interaction between the amino proton of (*S*)-**2** and the terminal carbonyl oxygen of (*S*)-**1**.

An enantiorecognition rationale based on NMR data in which an interaction model for both diastereoisomeric solvates was obtained [30] concerned the separation of enantiomeric 2′-(2-propoxy)-1,1′-binaphthyl-2-ol (**3**) on CSPs obtained by linking quinine or its derivatives to silica by means of the double bond. In this case quinine (**4**) was used as CSP soluble model (Fig. 2).

Quinine was able to induce relevant nonequivalences of binapthyl derivative protons in $CDCl_3$ solutions. In the presence of the chiral auxiliary different longitudinal relaxation times of the two isopropyl methyls of (*S*)-**3** were measured, whereas the relaxation parameter was not differentiated in the (*R*)-**3**/**4** mixture. The occurrence of an intermolecular hydrogen bond quinine-analyte was clearly demonstrated by the fact that addition of methanol to the mixtures made NMR parameters of the two enantiomers equal to that of pure binaphthyl derivative. Furthermore hydroxyl proton resonance of (*S*)-**3** was broadened by the presence of quinine to a larger extent than that of (*R*)-**3**. The most relevant information was gathered on the basis of NOE experiments, which allowed the authors to impose proximity constraints between selector and selectand protons. In particular differentiated NOEs were detected in the two mixtures. On these bases an interaction model (Fig. 2) was proposed in which the hydroxyl group of (*R*)-**3** produced attractive hydrogen bond interactions with quinine hydroxyl without causing significant repulsive steric interactions, unlike (*S*)-**3**/**4**, in which hydrogen bond interaction also involved steric repulsive interactions due to isopropyl protons and bulk quinine groups. The above interaction model, which suggested the enhanced stability of (*R*)-**3**/**4** adduct relative to (*S*)-**3**/**4** pair, was in keeping with elution order on the corresponding CSP.

It is noteworthy that frequently spectroscopic investigations regarding the soluble models of CSPs led to developing them as chiral solvating agents [31,32] for the determination of enantiomeric compositions by NMR, providing methods for the analytical separation of enantiomers which were complementary to chiral chromatography.

More recently, Pirkle's complex was modelled by Gasparrini and co-workers [33] by means of a computational protocol also involving the comparison between experimental and calculated NOE ratios, which underlined the relevance of conformational flexibility in the rationalization of macroscopic properties of the complex in solution.

Another example of NMR investigation of chiral recognition phenomena in which both diastereoisomeric complexes were characterized deals with the use of 9-*O*-acetyl (**5**) and 9-*O*-(3,5-dimethoxyphenylcarbamate) (**6**) quinines (Fig. 3) in the enantiorecognition of 2-(3,5-dinitrobenzamido)-1-phenylethanol (**7**) (Fig. 3) [10,34].

This study consisted of the following steps: (i) definition of the preferred conformation of the chiral auxiliary and the chiral substrate by NOE methods and analysis of the dependence of vicinal coupling constants on the dihedral angles; (ii) investigation of the self-association processes for both species, revealing that self-association processes of the chiral auxiliary **6** occurred, but with low values of the dimerization constants (<2 M^{-1}), making it possible to neglect them in the mixtures containing also the enantiomers of **7**: in this way the heteroassociation constants of the two diastereoisomeric species could be determined by progressive dilution procedures; (iii) on the basis of the values of the association constants of the two diastereoisomeric solvates, the optimal total concentration of the mixtures for having in solution a detectable amount of the complexed species was predetermined and the intra- and intermolecular NOE effects detected in order to obtain the prevailing conformations of the species constituting the two diastereoisomers. Thus, the interaction models of Fig. 3 were obtained, leading not only to the identification of the interactions responsible for the stabilization of the two diastereoisomeric solvates and those originating enantiodifferentiation, but also the precise nature of the conformational changes occurring as a consequence of the formation of the two complexes was shown.

Several other valuable papers described NMR investigations devoted to rationalizing enantiorecognition phenomena produced by quinine derivatives, in view of the applicative relevance of CSPs based on this class of chiral selectors [35–39].

No further examples will be described, as the cases discussed above well exemplify the NMR approaches which are required by small sized selectors.

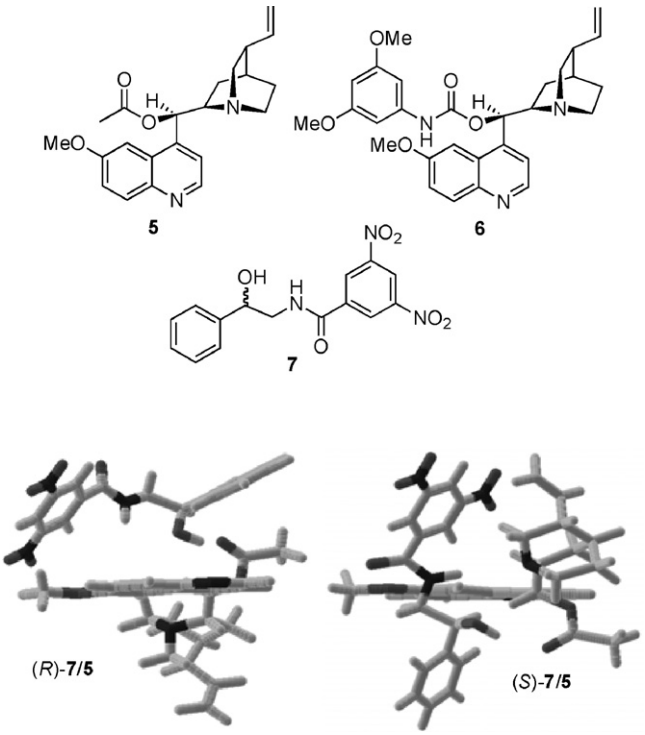

Fig. 3. Chiral auxiliaries **5**–**6** and analyte **7**. Representation of chiral recognition model for (*R*)-**7**/**5** and (*S*)-**7**/**5** adducts.

4. Cyclodextrins

Among presently applied chiral selectors, native or modified cyclodextrins are effectively used in the majority of enantioseparation techniques and, in spite of the fact that a large number of NMR investigations have addressed this class of chiral selectors, the mechanism of chiral discrimination is still not well understood.

Several exhaustive reviews were dedicated to the application of NMR methods to cyclodextrins and their complexes [23,40–44].

The propensity of cyclodextrins to include various organic compounds in their cavities is well ascertained [44]. However the main unanswered question regards the possibility that formation of inclusion complexes would not be a prerequisite for enantiorecognition. In this regard, Schurig reported [45,46] that racemic *N*-trifluoroacetyl-*O*-methyl esters of α-amino acids could be separated on both heptakis(2,3-di-*O*-acetyl-6-*O*-*tert*-butyldimethylsilyl)-β-cyclodextrin (AcSiCD7) and on the analogous acyclic dextrin counterpart heptakis[(1′-*O*,6-*O*)-*tert*-butyldimethylsilyl-(2,3-di-*O*,4″-*O*)-acetyl)]maltoheptaose (AcSiG7, G = glucose), as well as octakis[(3-*O*,-4″*O*)-butanoyl-(1′-*O*,2,6-di-*O*)-*n*-pentyl]maltooctaose (which was the open chain analogue of Lipodex E) gave rise to chromatographic enantioselectivity [47]. In above-mentioned cases enantiorecognition could be attributed to the presence of helical conformations in which "semicavities" are present.

Chankvetadze clearly addressed these topics in a very comprehensive review [23] in which he also pointed out that in view of multiple forces involved in analyte–CD interactions, combined molecular modelling-spectroscopy approaches are required in order to shed more light on the molecular basis of chiral recognition processes.

Other topics which must be addressed when dealing with cyclodextrins regard perturbation of their truncated cone shape which could occur when derivatizing groups are present on the large and/or small rims. The involvement of supramolecular aggregation in enantiorecognition processes should also be taken into consideration.

Much literature is dedicated to NMR investigations [23,40–44] regarding inclusion phenomena between chiral guests and cyclodextrins and inclusion can be very easily recognized by NMR by the simple comparison of complexation induced shifts of internal and external protons of the cyclodextrins in mixtures analytes/cyclodextrins. Protons H_3 and H_5, which respectively point at the large and small internal part of the cavity, are remarkably sensitive to the presence of guest molecules. Moreover, intense intermolecular NOE or ROE effects can be detected frequently between the same protons and nuclei of the included molecule. Comparison of the magnitudes of complexation induced shifts and NOE/ROE effects makes it possible to define the inclusion stereochemistry. Complexation parameters (stoichiometries and association constants) can be accurately determined by exploiting dependence of chemical shifts on molar ratios or total concentration and methods based on the detection of diffusion coefficients are also well suited. In spite of the very detailed stereochemical and thermodynamic information which are collected by NMR, it is very difficult to differentiate the stereochemistry of the two diastereoisomeric inclusion complexes. This is especially true for symmetrically substituted cyclodextrins, which give rise to enantiodiscrimination also in the presence of equal inclusion geometries: no significant stereochemical differentiation can be devised from the analysis of variations induced in chemical shifts or relaxation rates by cyclodextrins complexation or on the basis of NOE data. In fact, in the majority of cases only differences in the magnitudes of the above effects are detected, mainly reflecting differences in the thermodynamic stabilities of the two diastereoisomeric solvates formed in solution.

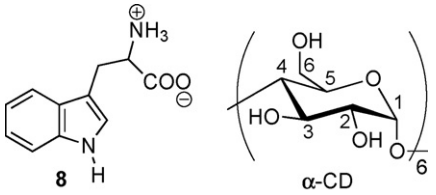

Fig. 4. Structures of guest (**8**) and α-cyclodextrin.

In 1992 Lipkowitz et al. [48] selected D,L-tryptophan (**8**) and α-cyclodextrin (α-CD) (Fig. 4) as a size consistent host–guest pair for which chromatographic enantioseparation was reported on α-CD chiral stationary phase [49] and investigated their enantioselective binding by NMR in water and by molecular dynamics simulations. The aim of this paper was not only to establish inclusion geometries and to compare association constants of the two diastereoisomeric inclusion complexes, but also to point out differential interactions between the host and the two enantiomeric guests that could explain enantiodiscrimination.

Firstly, conformation of free amino acid was established by 1D-difference NOE experiments, which was inconsistent with the solid-state structure. Based on time-averaged NMR data, cyclodextrin structure did not show any asymmetry, contrary to computational results [50]. In the mixtures (*R*)- or (*S*)-**8**/α-CD, complexation shifts were measured which were greater for the (*R*)-enantiomer than they were for the (*S*), according to chromatographic retention data. Also relaxation T_1 parameters showed a decrease in the mixture relative to pure compounds, but T_1 values of amino acid in the mixtures remained higher with respect to T_1 of cyclodextrin. Thus, tryptophan, though complexed, still reoriented faster than cyclodextrin. A proximity constraint between indole aromatic proton of both enantiomers and internal H_3 proton of α-CD located on the large part of the internal surface was imposed on the basis of NOE data, which revealed that amino acid was included, but not deeply embedded in the cyclodextrin. Thus no detectable differences between the two diastereoisomeric inclusion complexes were obtained by NMR and only gas-phase molecular simulations revealed that (*R*)-**8** formed a larger number of hydrogen bonds than did (*S*)-**8**; the intermolecular hydrogen bonds are produced by the tryptophan carboxylate oxygens and its indole N–H rather than by the ammonium group. In this way inclusion as a prerequisite of chiral discrimination was shown, in accordance with what was proposed by Armstrong [51].

To investigate binding of a typical, neutral chiral guest associating with β-cyclodextrin (β-CD), methyl mandelate (**9**) (Fig. 5), which was expected to have weaker hydrogen bonding to the cyclodextrin than zwitterion tryptophan, was selected by the same author [52] and a solvent mixture (CD_3OD/D_2O = 4:96) consistent with chromatographic experimental conditions was employed for NMR analyses.

On complexation, internal H_3 proton, located on the large internal part of the cavity, experienced the largest induced low-frequencies shift, indicating that it resides in the cone of shielding

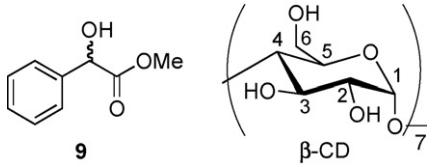

Fig. 5. Structures of guest (**9**) and β-cyclodextrin.

produced by the methyl mandelate aromatic ring, which is embedded in the cyclodextrin cavity. ^{1}H nuclei nonequivalence was not detected and the only non-isochronous chemical shifts found are from the ^{13}C methyl resonances in the binary complexes. Complexation induced shifts of ^{13}C nuclei demonstrated that (*S*)-**9** was more tightly bound to the cyclodextrin relative to (*R*)-**9**, both located in proximity to the secondary rim of the β-CD, as revealed by weak intermolecular NOEs. However stereochemical differentiation of the two diastereoisomeric solvates remained unresolved once again. Computational methods demonstrated that while the shapes of the complexes are similar, the more stable diastereoisomer is more compact than the less stable complex.

The ordered network of hydrogen bonds between the secondary hydroxyl groups of adjacent rings of underivatized cyclodextrins, which determines the global truncated cone shape, is strongly perturbed by the presence of derivatizing groups: more flexible structures are obtained due to the loosening or breaking of the hydrogen bond belt which causes dramatic changes in their complexing and enantiodiscriminating properties. Bulky benzoyl derivatizing groups on the secondary sites of α-CD led to a symmetry change from C_6 to C_3 which was clearly detected in the ^{1}H NMR spectra recorded in $CDCl_3$: two sets of resonances were observed corresponding to two different kinds of glucopyranose rings [53,54]. In several cyclodextrin derivatives no such symmetry changes can be detected by NMR and only time-averaged NMR spectra are obtained. However a suitable protocol of analysis of their conformational features can be employed [55–57], based on the determination of cross-relaxation parameters of selected proton pairs of glucopyranose rings. Significant rotation about glycosidic linkages and the presence of skewed glucopyranose rings were demonstrated in the case of peracetyl-β-cyclodextrin [56], as well as for several other kinds of cyclodextrin derivatives in which hydrogen bond donor groups are absent on the secondary sites [57]. These assessments were based on the comparison of intraglucose H_1–H_2 and interglucose H_1–$H_{4'}$ ROEs: in undistorted situations ROE H_1–$H_{4'}$ is expected to be more intense than H_1–H_2 (Fig. 6a). When rotations about the glycosidic linkages occur, then a lengthening of H_1–$H_{4'}$ distance is observed relative to the fixed H_1–H_2 distance (Fig. 6b) and the two ROEs become comparable.

Rotation is also well reflected in detection of true ROEs between H_1 proton of one unit and H_3 and H_5 internal protons of the adjacent unit. The same kind of analysis was performed by comparing cross-relaxation rates of H_1–$H_{4'}$ and H_1–H_2 proton pairs, from which the corresponding interproton distances were calculated. Cross-relaxation parameters were obtained by measuring mono- and biselective relaxation rates (see NMR methods).

Enantioselective inclusive processes by cyclodextrin derivatives were reported already in 1992 by König and co-workers [58], who described the interaction of (*R*,*S*)-methyl-2-chloropropionate (**10**) with heptakis(3-*O*-acetyl-2,6-di-*O*-pentyl)-β-cyclodextrin (Lipodex D, Fig. 7). NMR spectra recorded in cyclohexane-d_{12} showed very high differentiation of methine protons of enantiomeric **10**, which were also significantly differentiated in linewidth. Complexation shifts were in accordance with GC retention data and a chiral recognition rationale was devised on the basis of molecular dynamics simulations.

Derivatizing groups may generate an enlarged cavity, may direct interactions towards the external surface of the cyclodextrins [54,57,59–61] or lead to self-inclusion of functional groups [62]. Thus permethylated-β-cyclodextrin did not show in CD_3OD solution any propensity to include chiral apolar substrates such as trisubstituted allenes [63], for which, in principle, inclusion should have been the favoured complexation pathway. No dipolar interactions were shown between chiral allenes protons and internal protons of the cyclodextrin. Moreover the chemical shifts of cyclodextrin internal protons remained unchanged on complexation. By contrast, some intermolecular dipolar interactions were obtained with external protons of the cyclodextrin. Thus NMR measurements showed that inclusion was not a complexation pathway needed for enantiodiscrimination. In spite of the fact that association constants of diastereoisomeric complexes were very low and nearly equal, very high NMR anisochrony of allenes protons was detected [63,64]. The above result confirmed that subtle time-averaged stereochemical differentiation of the two diastereoisomeric solvates contribute to differentiating them. Probably supramolecular aggregation phenomena involving diasteroisomeric solvates, which are not able to give rise to detectable thermodynamic differentiation, are sufficient for NMR differentiation.

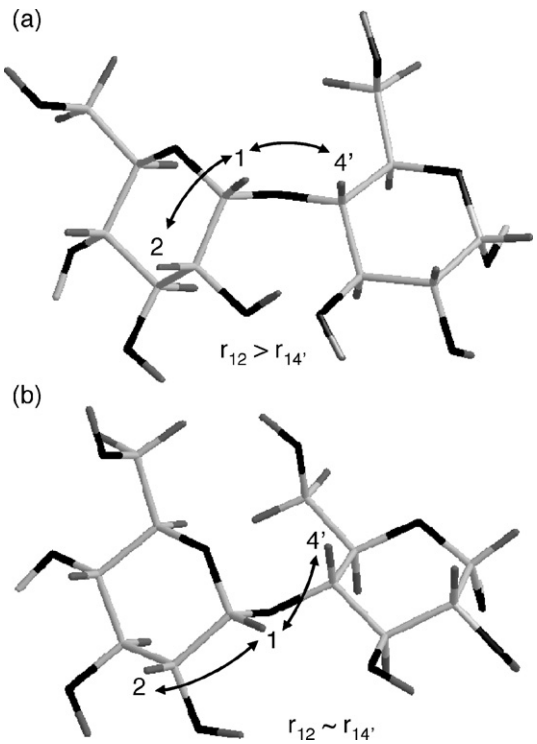

Fig. 6. Representation of two adjacent glucose units in undistorted arrangement (a) and distorted arrangement (b) due to the rotation around the glycosidic linkage.

Chankvetadze reported [65] the separation of twenty-three cationic chiral analytes in capillary electrophoresis using native β-CD and heptakis(2-*O*-methyl-3,6-di-*O*-sulfo)-β-cycloclextrin (HMdiSu-β-CD) (Fig. 8) as chiral selectors and the structure of cyclodextrin-analyte complexes in aqueous solution were investigated using one-dimensional transverse rotating frame nuclear Overhauser and exchange spectroscopy.

It was found that external complexes are formed by analytes **11**, **12** and **13** shown in Fig. 8, as some intermolecular ROEs between their protons and OCH_3 groups of HMdiSu-β-CD, which are located on the secondary rim of the cavity, were detected. Despite external analyte–selector interactions, quite strong complexes were

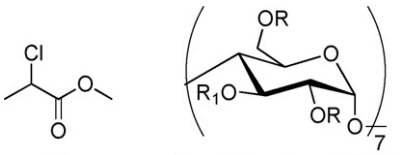

10 $R = C_5H_{11}$ $R_1 = COCH_3$ Lipodex D

Fig. 7. Structures of analyte (**10**) and cyclodextrin derivative Lipodex D.

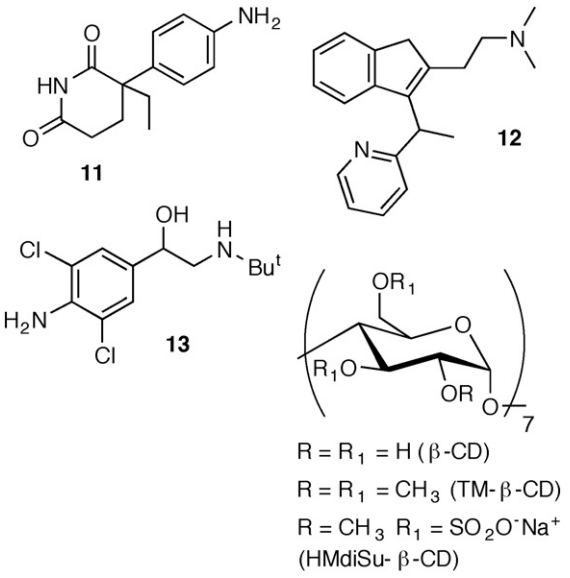

Fig. 8. Structures of analytes **11**–**13** and cyclodextrin selectors β-CD, TM-β-CD and HMdiSu-β-CD.

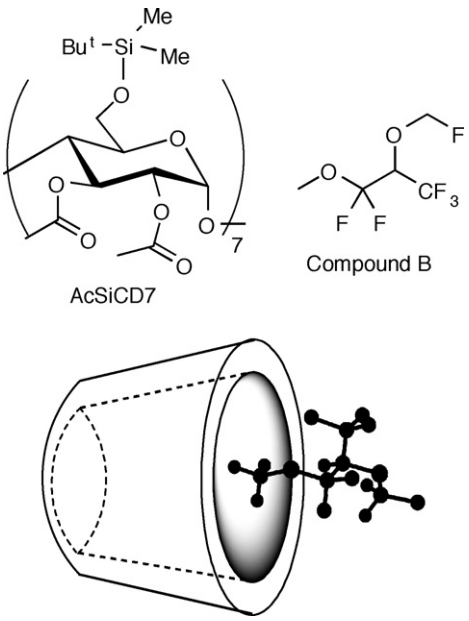

Fig. 9. Structures of compound B and chiral selector AcSiCD7. Graphical model showing partial inclusion of guest in the host cavity.

formed in these cases, confirming that enantiodiscrimination was not necessarily determined by inclusion and strong complexes can originate also from interactions occurring at the external surface of the cyclodextrin. The above data confirmed previous observations based on chromatographic data [66].

An interesting case is represented by the chromatographic separation of the 1,1,1,3,3-pentafluoro-2-(fluoromethoxy)-3-methoxypropane (compound B), a chiral degradation product of the inhalation anaesthetic sevoflurane, on heptakis(2,3-di-*O*-acetyl-6-*O*-*tert*-butyldimethylsilyl)-β-cyclodextrin (AcSiCD7) as chiral selector. AcSiCD7 gave a very high separation factor of 4.08 for racemic compound B, which dropped to 2.70 for the γ-cyclodextrin analogue AcSiCD8 and no enantioseparation at all was obtained for α-CD analogue AcSiCD6 [45]. Surprisingly, the separation of compound B occurs also on the corresponding open chain selectors AcSiG7 and AcSiG8 [45].

NMR investigations [67] demonstrated that in apolar solvents AcSiCD7 originated very high NMR anisochrony of the two enantiomers of compound B (Fig. 9), which was due to formation of 1 to 1 diastereoisomeric solvates with association constants, calculated on the basis of DOSY experiments, of 48 M^{-1} for (*R*)-enantiomer complex and about 72 M^{-1} for (*S*)-one, in accordance with chromatographic retention data.

ROE measurements demonstrated that both enantiomers were not deeply inserted into the cyclodextrin as only inter-ROE with internal protons H_3 of AcSiCD7 located on the large cavity part was detected together with several dipolar interactions between enantiomeric substrates and external silyl groups located on the primary sites. The basis of this behaviour must be sought in the conformational features of AcSiCD7: the use of the suitable NMR protocol of conformational analysis [56,57] revealed that significant rotation about glycosidic linkages and deviations from the $^4C_1$ chair structures occurred [67]. Both factors made silyl groups on the primary sites in the proximity of secondary ones and, hence, attractive fluorine-silicon interactions between fluorinated groups of chiral substrates protruding from the large rim and silyl groups on the primary sites were favoured, which allowed chiral substrate to be included, but not deeply. Probably enantiodiscrimination was the result of multiple attractive interactions at the internal and external surface, which cooperated more efficiently in the complex formed by (*S*)-B than they did in (*R*)-B/AcSiCD7 complex. The relevance of superficial fluorine–silicon interactions was confirmed by the ability of analogous acyclic oligosaccharides, for which inclusion is not possible, to enantiodiscriminate compound B although with minor enantiodiscriminating efficiency [45].

Recently Wimmer and co-workers [68] examined the interaction between the same fluorinated compound B and Lipodex E (Fig. 10) or its β-analogue.

In this case NOEs were detected between fluorine nuclei and both H_3 and H_5 internal protons, which supported the deep inclusion of the substrate; association constants were high and remarkably differentiated for the γ-selector and lower for the β-analogue, indicating a strong dependence on the cavity size. Hence the authors were surprised that acetylated-silylated cyclodextrins did not behave in a similar way in the interaction with compound B [67], overlooking the fact that derivatizing groups, as clearly pointed out in several cases [60,61], are able to direct interactions towards the external surface of the cyclodextrin at the expense of inclusion. This is particularly true in the case of silylated-acetylated cyclodextrins and fluorinated analytes by virtue of the strong silicon–fluorine affinity.

NMR experiments [69] confirmed the ability of acyclic acetylsilyl-oligosaccharides to interact enantioselectively with other kinds of fluorinated substrates and demonstrated that inclusion is not a prerequisite for enantiodiscrimination.

The effect of derivatization on the depth of inclusion has also been demonstrated by Chankvetadze who showed with ROE experiments that *N*,*N*-dimethyl-2-[1-(1-pyridin-2-ylethyl)-3H-inden-2-yl]ethanamine) (dimethindene, **12**) [70] does not enter

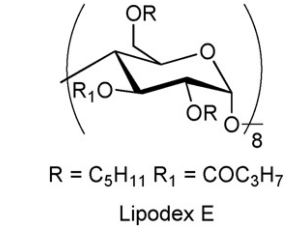

Fig. 10. Structure of chiral selector Lipodex E.

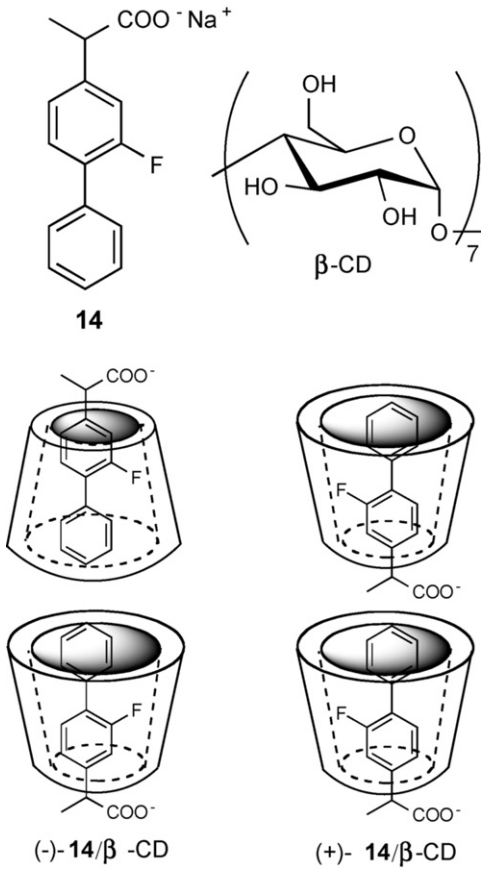

Fig. 11. Structures of flurbiprofen (**14**) and β-cyclodextrin and graphical representation of diastereoisomeric supramolecular aggregates.

the cavity of permethylated-β-CD (TM-β-CD) as deeply as the cavity of β-CD (Fig. 8). Different inclusion features were the basis for explaining different affinities shown by the two enantiomeric analytes in CE and were well supported by the values of the binding constants determined using NMR spectroscopy.

The relevance of supramolecular aggregation processes in enantiodiscrimination by underivatized β-CD was demonstrated by NMR in the case of the two enantiomers of flurbiprofen (**14**) [71] (Fig. 11): anisochrony of enantiomers resonances was observed in D_2O solution, with relevant low-frequencies shifts of internal protons H_3 and H_5 of the cyclodextrin due to anisotropic effects of aromatic moieties of deeply included substrates.

The continuous variation method supported the formation of 1:1 diastereoisomeric complexes, association constants of which were determined by using the Benesi–Hildebrand approach modified for NMR. Inclusion processes were also demonstrated by ROE measurements. However the most interesting effect regarded the slowing down of molecular motion of the cyclodextrin in the presence of both enantiomers, which was surprising as formation of inclusion complexes is expected to affect the dynamics of included analytes only. The above-mentioned change in motional features was detected by comparing cross-relaxation parameters of the proton pair H_3–H_5 located inside cyclodextrin cavity in the pure host and in the presence of analytes enantiomers. Intermolecular dipolar interactions were in agreement with the presence of supramolecular aggregates of complexes which are head-to-tail for one enantiomer and head-to-head for the other one (Fig. 11). This observation was supported by the X-ray analysis of complexes formed by racemic **14** and β-CD, showing a similar head-to-head pairing [72].

5. Polysaccharides

Polysaccharide derivatives are the basis of the most widely used CSPs, however enantiorecognition rationales, which were proposed for such a class of chiral selectors, are still elusive. Full exploitation of NMR potentials was made difficult by several problems such as very low solubility of polymeric materials in NMR solvents, which do not compete with enantiomeric substrates in the interaction with polymeric matrix. Polar solvents in which polysaccharides have good solubilities destroy enantiomeric interactions. Furthermore, in several cases the structure of the chiral selector, i.e. the polymer, is not well defined.

Okamoto and Yashima gave a fundamental contribution in this area [73–78]. In consideration of the applicative relevance of CSPs based on phenylcarbamate derivatives of cellulose and amylose, they explored different kinds of polymer derivatives which combined chromatographic efficiency and good solubility in NMR solvents like $CDCl_3$. Cellulose tris(5-fluoro-2-methylphenylcarbamate) (**15**) (Fig. 12) had both requirements and was employed in NMR enantiodiscrimination experiments of 1,1′-bi-2-naphthol (**16**) and 2,2′-dihydroxy-6,6′-dimethylbiphenyl (**17**) (Fig. 12). The polymer produced very high chemical shift differentiation of enantiomeric substrates, as well as large separation factors in HPLC.

(*S*)-**16** hydroxyl proton resonance was significantly shifted to high frequencies by 0.4 ppm in the presence of the polymer. Deshielding was remarkably higher than it was for (*R*)-**16**. Hydroxyl deshielding, which was attributed to hydrogen bond interactions with polysaccharide polar groups, was accompanied by significant low-frequencies shifts of some (*S*)-**16** aromatic protons ascribed to stacking interactions with polysaccharide aromatic derivatizing groups. Noticeably NMR results were consistent with chromatographic enantioseparation using the same polysaccharide. Lack of one or both hydroxyl groups as in **18** (Fig. 12) destroyed NMR enantiodiscrimination, showing the role of hydrogen bond interactions. In the mixture **15**/(*S*)-**16** some intermolecular dipolar interactions imposed proximity constraints between selected aromatic protons of (*S*)-**16** and methyl groups of polysaccharide, also allowing the authors to differentiate the extent of interaction with the three different derivatization sites on the glucose moieties. ^{13}C spin-lattice relaxation rates of (*S*)-**16** in the presence of **15** underwent significant reductions, demonstrating slowing down of molecular motion of enantiomeric substrate due to the interaction with the polysaccharide. Interestingly T_1 reduction was greater for naph-

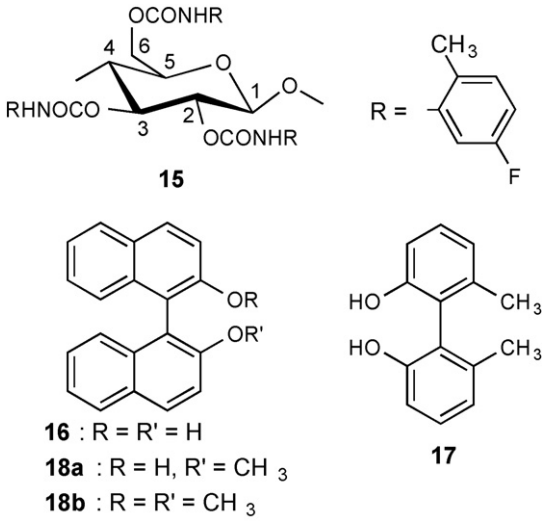

Fig. 12. Structures of polysaccharide derivative **15** and analytes **16**–**18**.

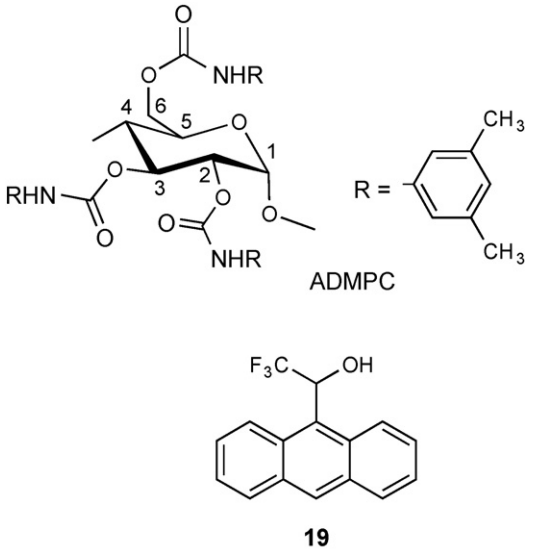

Fig. 13. Structures of amylose derivative ADMPC and analyte **19**.

thyl carbons adjacent to hydroxyl groups, indicating the relevance of hydrogen bond interactions probably with carbonyl groups of carbamate. An accurate analysis of thermodynamic parameters was also performed by ^{1}H NMR titration experiments in which dependence of chemical shifts of **16** in **16**/**15** mixtures was analysed both by linear and non-linear fittings. Very similar results were obtained on the basis of chemical shift variations of different protons. NMR experiments showed another interesting feature as OH proton resonance disappeared during the time for (*R*)-**16** and remained observable for (*S*)-**16**, probably due to the different H_2O exchange behaviour, which was hindered in the (*S*)-enantiomer which was more tightly bound to polysaccharide. Water exchange was more favoured for (*R*)-**16**. Finally titrations of **15** with (*S*)- and (*R*)-**16** were also performed showing the relevant low-frequency shift of ring proton H_2, leading to the more precise location of the interaction site on the polysaccharide glucose residues. Comprehensive NMR approach and HPLC data were combined to structural X-ray data of cellulose tris(phenylcarbamate) (CTPC) [79,80] to conclude by a molecular modelling approach that polysaccharide is in a helical conformation with polar carbamate groups located inside polymer chain and hydrophobic aromatic groups outside it so that polar enantiomers can get into the groove to interact with the carbamate residues *via* hydrogen bonding formation. Enantiodiscrimination was attributed to the ability of (*S*)-**16** to involve both hydroxyl groups in the interaction with carbonyl moieties of polysaccharides, whereas for (*R*)-**16** only the involvement of a single hydroxyl group is possible. Okamoto and co-workers [73] also demonstrated by NMR experiments the role of polar additives, such as 2-propanol.

Amylose phenylcarbamates, as corresponding cellulose derivatives, showed very high enantiorecognition capabilities in HPLC, but these polymers were soluble only in polar solvents and their X-ray structure was not known, thus NMR experiments were performed [81] on low-molecular-weight amylose tris(3,5-dimethylphenylcarbamate) (ADMPC) (Fig. 13), which was soluble in chloroform and exhibited chiral discrimination toward many enantiomers in NMR as well as in HPLC.

To propose a structure for ADMPC, Buchanan's method [82] was exploited, in which the interproton distances of the glucose protons were defined by NOESY experiments among which inter-ring H_1–$H_{4'}$ distances were related to the torsion angle about the glycoside bond. For ADMPC selected fixed proton distances (H_2–H_4 and H_3–H_4) in the same glucose unit were used as the internal reference. NMR data were coupled with computer modelling, and a left-handed helical structure was obtained as the most probable one for polysaccharide.

NMR enantiodiscrimination experiments [81] were performed by using ADMPC as chiral solvating agent in chloroform solutions and compared to HPLC separations on a CSP with ADMPC chemically bonded to silica which allowed the authors to use chloroform as the eluent. 1-(9-Anthryl)-2,2,2-trifluoroethanol enantiomers (**19**) (Fig. 13) were used as probe substrates to investigate chiral discrimination mechanism. Significant shielding of selected protons of the glucose units of ADMPC as the consequence of the presence of (*S*)-**19** indicated that its anthryl ring may be closely located above these protons. The effect of (*R*)-**19** on chemical shifts of the same glucose protons was negligible. A model of chiral discrimination was proposed gathering together NMR, HPLC and molecular modelling results.

6. Chiral micelles

Several contributions can be found in the literature regarding NMR investigations on modifiers for electrokinetic chromatography (EKC) based on micellar systems [83–92].

In a review published in 2005 [93] Morris cast light on the role of NMR spectroscopy in the elucidation of intermolecular interactions relevant in separations conducted with EKC, in which run buffer contains a modifier that interacts with analytes. In micellar EKC (MEKC) the modifier is a surfactant which behaves as a pseudostationary phase and separations are based on the different affinities of analytes for micelles. Even though complexation phenomena responsible for enantiodiscrimination can be elucidated by exploiting NMR methods analogous to those described in the previous sections, the formation of micellar aggregates raises the problem of exploring also the real nature of the chiral selector or their aggregation processes.

In this last regard, an interesting NMR investigation was reported regarding the use of sodium cholate (SC) as pseudostationary phase modifier [83] in capillary electrophoresis for chiral recognition of rigid analytes such as (*R*,*S*)-1,1′-binaphthyl-2,2′-diylhydrogenphosphate ((*R*,*S*)-BNDHP) (Fig. 14).

Bile acids are rigid, planar steroidal compounds, which by virtue of the directionality of their hydroxyl groups and the presence of steroid skeleton, are amphipathic molecules able to form aggregate micellar structures as a function of concentration. A very good correspondence was found between mobilities of (*R*,*S*)-BNDHP in MEKC and chemical shifts of ^{31}P nuclei.

In the presence of SC above the first critical micelle concentration (e.g., >14 mM), enantioselective association with the cholate micelle results in chiral resolution of (*R*)- and (*S*)-BNDHP by MEKC and it is observed that the (*S*)-isomer has a longer retention time than the (*R*)-isomer, indicating a longer residence time for the (*S*)-isomer in the micelle. ^{31}P NMR chemical shifts

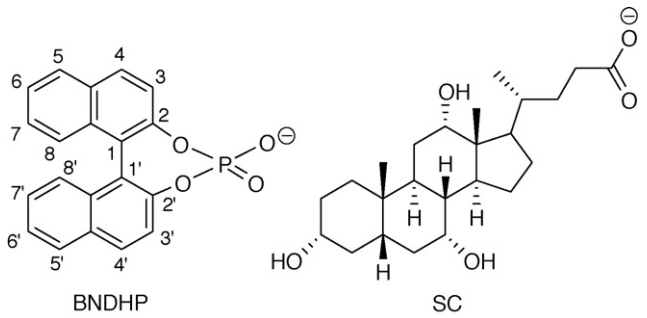

Fig. 14. Structures of analyte BNDHP and SC.

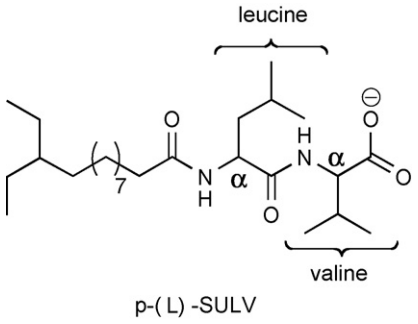

Fig. 15. Structure of p-(L)-SULV.

of the analytes were perturbed by the presence of SC starting from 7 mM cholate with an inflection point at 14 mM cholate. Chemical shifts of (*S*)-BNDHP were more perturbed by cholate with respect to (*R*)-enantiomer. However, the (*S*)-isomer chemical shift was more strongly perturbed in the racemate than when enantiopure. Therefore (*R*)-BNDHP enhanced the fraction of micelle-bound (*S*)-BNDHP, giving rise to a kind of allosteric effect. This fact demonstrated that micelles are able to simultaneously accommodate (*R*)- and (*S*)-isomers. The authors reported [83] that the ratio between spin–lattice (T_1) and spin–spin (T_2) relaxation time constants for the ^{31}P nucleus was very sensitive to the change in cholate aggregation caused by concentration gradients. In particular, significant changes in the T_1/T_2 ratio were observed beginning at 5 mM sodium cholate, with an abrupt level at 50–60 mM. Chemical shifts of the different protons of (*R*,*S*)-BNDHP were also useful evidence of the aggregation processes and binding interactions between BNDHP and the cholate micelle. In fact different kinds of cholate aggregates were sampled by different protons of BNDHP.

Among polymeric modifiers, spectroscopic investigations have focussed on poly(sodium *N*-undecanoyl-L-leucylvalinate) [p-(L)-SULV] (Fig. 15), which has shown a 77% overall success rate in separating a randomly chosen group of 75 neutral, cationic, and anionic drug compounds [84,85].

Its interaction with analytes was studied by NOE and diffusion methods. NOE measurements led to imposing proximity constraints which demonstrated analyte partitions between the chiral polar head-groups of the molecular micelle and the hydrophobic core. This was in agreement with chiral CE theory which suggests that hydrophobic analytes undergo rapid mass transfer into and out of the pseudostationary phase. For every (*S*)-BNDHP proton a stronger NOE was observed for the proton bound to the chiral centre of leucine fragment of p-(L)-SULV, whereas selected protons of (*R*)-BNDHP showed stronger NOEs to protons of valine fragment. Thus not only were primary interaction sites of the two enantiomers defined by NMR, but they were also differentiated for the two enantiomers.

To shed some light on the origin of the synergic behaviour of the mixed micellar systems of sodium dodecyl sulphate (SDS) and sodium cholate, employed to obtain enhanced versatility in the chromatographic separation of corticosteroids [86], two classes of NMR parameters were measured: self-diffusion coefficients and ^{2}H relaxation parameters R_1 and R_2 for specifically ^{2}H labeled (in the α-position) SDS. The addition of cholate to the SDS solution decreased the fraction of monomeric SDS, as indicated both by the increase in the relaxation parameters and the decrease in the SDS self-diffusion coefficients. When the diffusion and relaxation rates level out, the amount of free SDS was negligible. Further addition of cholate had little effect on the micellar size, as shown by the constancy in the SDS diffusion coefficients and in the value of ΔR.

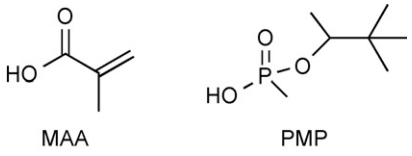

Fig. 16. Structures of MAA and PMP.

7. Molecularly imprinted polymers (MIPs)

Molecularly imprinted polymers (MIPs) are synthetic polymers having a predetermined selectivity for a given analyte, or a group of structurally related compounds. The most widely used technique for preparing MIPs is non-covalent imprinting, in which the complex of template and functional monomer is formed *in situ* by non-covalent interactions. Due to the nature of the support, only complexation phenomena occurring during the prepolymerization phase can be suitably investigated by NMR spectroscopy [94–99]. However a relevant contribution to a more efficient MIP design may arise from NMR titration experiments: self-aggregation propensities of monomers can be established depending on the nature of the solvent employed and stoichiometries and association constants of the complexes monomer/template can be determined. For a complete analysis the role of cross-linker can also be established.

Recently Palmas and co-workers reported [97] a work whose aim was the rational design of methacrylic acid (MAA)-based non-covalently imprinted polymers in which pinacolyl methylphosphonate (PMP) was employed as template (Fig. 16).

The authors employed molar ratio method to determine PMP and MAA complexation stoichiometry. The molar ratio method was also the basis for the determination of association constants. MAA self-aggregation, which is of primary importance in the template monomer prearrangement step, was investigated with different procedures of fitting of dilution data and MAA dimerization constants of 8 M^{-1} and 0.3 M^{-1} were respectively calculated in toluene-d_8 and CD_3CN/toluene-d_8. Thus solvent mixture was chosen for studying heteroaggregation phenomena of MAA and PMP. Interestingly, the above mixture of solvents was known to give rise to highly porous MIPs [100]. For the determination of MAA/PMP association constants no assumption regarding complexation stoichiometry was made and, only on the basis of the hypothesis that a single complexed form prevails in solution, complexation stoichiometry and association constants were simultaneously determined by using the fitting approach described by Ramirez and co-workers [101]. In this way a 1:1 stoichiometry was established with an association constant of 1.4 M^{-1}, which is in keeping with the formation of a single hydrogen bond between the monomer and the template. Taking into account that the aim of this work was to develop a high affinity MIP, in which nonspecific interactions are minimized, NMR results were used as the basis for preparing an MIP starting from 1:1 PMP/MAA ratio instead of the conventional 1:4 ratio.

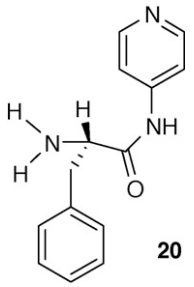

Fig. 17. Structure of template **20**.

For a molecularly imprinted polymer employing 4-L-phenylalanylamino-pyridine (**20**) (Fig. 17) [102] the significant changes in the line widths of the exchangeable proton of the amino group were used as a basis for establishing the formation of two different complexes with MAA monomer, with 1:1 and 1:2 stoichiometries respectively.

8. Conclusions

The molecular basis of enantiorecognition phenomena involved in chromatographic separation technologies can be investigated in a comprehensive and direct way by exploiting the versatility of NMR spectroscopy.

Several size-dependent phenomena can be detected by NMR such as translational diffusion or reorientational motions in solution, which are strongly affected by complexation processes and reflect analytes-selectors affinities. Such global parameters make it possible to ascertain thermodynamic contributions to enantiorecognition phenomena. The stereochemical basis of chiral recognition can be ascertained very precisely by NOE or ROE methods which provide proximity constraints that are very useful for exploring interactions responsible for enantiorecognition. Preliminary information in this regard can be also obtained by the simple analysis of complexation induced shifts which are determined by comparing routine NMR spectra of the pure selectors or analytes and their mixtures. This last approach also constitutes the basis for developing NMR methods of determination of enantiomeric purities which are complementary to chromatographic techniques. In fact, several chiral solvating agents were modelled on chromatographic selectors.

Some aspects must be taken into consideration in comparing chiral recognition models based on NMR results with chromatographic data. In fact, the efficient differentiation of NMR nuclei of enantiomeric substrates in the presence of chiral selectors does not require high selector–selectand affinity or significant differentiation of association constants of diastereoisomeric solvates [63].

In the CE techniques a difference in the mobilities of free and complexed analytes is required to observe a separation [103,104] and, much like NMR, high thermodynamic differentiation is not a prerequisite. The different contributions to separations in CE versus NMR were, in fact, clearly highlighted in cases where the change of CE experimental conditions led to a change in the migration order that failed to produce changes in the positions of NMR signals [103,104]. Thermodynamic differentiation is a prerequisite in other chromatographic techniques.

Beyond the above warnings, a very good fit between enantiorecognition mechanisms obtained by NMR investigations and chromatographic data is expected in the case of electrophoretic technologies. More care should be taken in devising chromatographic enantiorecognition rationales by NMR when the chiral auxiliary is linked to solid supports: some interactions could occur at the solid achiral support and chiral auxiliary could also undergo unpredictable conformational changes.

However, very precise interaction models for small sized chiral selectors can be obtained by comparing stereochemical and thermodynamic features of diastereoisomeric complexes formed in solution. In this way a significant contribution to knowledge of chiral recognition can be achieved, that is very useful for the rational design of improved selectors for chiral chromatography.

Symmetrical macrocyclic chiral hosts limits the possibility of differentiating diastereoisomeric solvates and the combined use of computational methods might be required. However, also for this class of chiral selectors, several aspects of complexation phenomena can be investigated; such as analytes-selectors relative stereochemistry. By NMR complexation phenomena involving deep inclusion, partial inclusion with cooperative interactions at the external surface, or interactions totally occurring at the external surface can be discriminated. Furthermore several relevant conformational features of chiral hosts can be precisely identified.

Knowledge of the stereochemistry of polymeric materials requires the combined use of NMR, X-ray crystallographic data and computational methods, from which the conformation in solution can be established. Thus, polymer-selectands proximity constraints obtained by NOE methods make possible the development of chiral recognition rationales to be compared to chromatographic data.

The use of chiral micellar modifiers as in MEKC generates an additional problem regarding the aggregation states of micelles, which can be solved by NMR by using probe molecules interacting with them or by measuring size-sensitive NMR parameters.

Finally, the potentialities of NMR spectroscopy in the rational design of molecularly imprinted polymers cannot be neglected given the tools it offers for the analysis of all aspects of the complexation phenomena involving the monomer, the template and also the cross-linker at the prepolymerization level.

Acknowledgment

The work was supported by the MIUR (FIRB Project RBPR05NWWC).

References

[1] W.H. Pirkle, T.C. Pochapsky, J. Am. Chem. Soc. 108 (1986) 5627.
[2] D. Neuhaus, M.P. Williamson, The Nuclear Overhauser Effect in Structural and Conformational Analysis, VCH, New York, 1989.
[3] L. Fielding, Tetrahedron 56 (2000) 6151.
[4] L. Fielding, Prog. Nucl. Magn. Reson. Spectrosc. 51 (2007) 219.
[5] P. Stilbs, Prog. Nucl. Magn. Reson. Spectrosc. 19 (1987) 1.
[6] C.S. Johnson Jr., Prog. Nucl. Magn. Reson. Spectrosc. 34 (1999) 203.
[7] G.A. Morris, Diffusion-ordered spectroscopy (DOSY), in: D.M. Grant, R.K. Harris (Eds.), Encyclopedia of Nuclear Magnetic Resonance, vol. 9, 2002, pp. 35–44.
[8] F. Aradi, A. Földesi, Magn. Reson. Chem. 25 (1987) 892.
[9] G. Uccello-Barretta, L. Di Bari, P. Salvadori, Magn. Reson. Chem. 30 (1992) 1054.
[10] G. Uccello-Barretta, F. Balzano, C. Quintavalli, P. Salvadori, J. Org. Chem. 65 (2000) 3596.
[11] D. Zuccaccia, A. Macchioni, Organometallics 24 (2005) 3476.
[12] H.C. Chen, S.H. Chen, J. Phys. Chem. 88 (1984) 5118.
[13] E.J. Cabrita, S. Berger, Magn. Reson. Chem. 39 (2001) S142.
[14] L. Allouche, A. Marquis, J.-M. Lehn, Chem. Eur. J. 12 (2006) 7520.
[15] K. Kaszynska, E. Banachowicz, G. Slósarek, A. Morawiec, I. Gawrońska, J. Barciszewski, J. Solution Chem. 31 (2002) 987.
[16] R. Wimmer, F.L. Aachmann, K.L. Larsen, S.B. Petersen, Carbohydr. Res. 337 (2002) 841.
[17] J. Homer, M.C. Perry, J. Chem. Soc. Faraday Trans. 1 82 (1986) 533.
[18] M.W. Hanna, A.L. Ashbaugh, J. Phys. Chem. 68 (1964) 811.
[19] R. Foster, C.A. Fyfe, Trans. Faraday Soc. 61 (1965) 1626.
[20] R.L. Scott, Recl. Trav. Chim. Pays-Bas 75 (1956) 787.
[21] S. Simova, S. Berger, J. Incl. Phenom. Macrocycl. Chem. 53 (2005) 163.
[22] L. Thunberg, S. Allenmark, Tetrahedron: Asymmetry 15 (2004) 1507.
[23] B. Chankvetadze, Chem. Soc. Rev. 33 (2004) 337.
[24] N. Niccolai, G. Valensin (Eds.), Advanced Magnetic Resonance Techniques in Systems of High Molecular Complexity, Birkhäuser, Boston, 1986.
[25] R. Freeman, S. Wittekoek, J. Magn. Reson. 1 (1969) 238.
[26] M. Karplus, J. Am. Chem. Soc. 85 (1963) 2870.
[27] C. Altona, M. Sundaralingam, J. Am. Chem. Soc. 95 (1973) 2333.
[28] W.H. Pirkle, T.C. Pochapsky, J. Am. Chem. Soc. 109 (1987) 5975.
[29] W.H. Pirkle, T.C. Pochapsky, G.S. Mahler, R.E. Field, J. Chromatogr. 348 (1985) 89.
[30] P. Salvadori, C. Rosini, D. Pini, C. Bertucci, P. Altemura, G. Uccello-Barretta, A. Raffaelli, Tetrahedron 43 (1987) 4969.
[31] W.H. Pirkle, A. Tsipouras, Tetrahedron Lett. 26 (1985) 2989.
[32] C. Rosini, G. Uccello-Barretta, D. Pini, C. Abete, P. Salvadori, J. Org. Chem. 53 (1988) 4579.
[33] S. Alcaro, F. Gasparrini, O. Incani, L. Caglioti, M. Pierini, C. Villani, J. Comput. Chem. 28 (2007) 1119.
[34] G. Uccello-Barretta, F. Balzano, P. Salvadori, Chirality 17 (2005) S243.
[35] N.M. Maier, S. Schefzick, G.M. Lombardo, M. Feliz, K. Rissanen, W. Lindner, K.B. Lipkowitz, J. Am. Chem. Soc. 124 (2002) 8611.
[36] C. Czerwenka, M.M. Zhang, H. Kählig, N.M. Maier, K.B. Lipkowitz, W. Lindner, J. Org. Chem. 68 (2003) 8315.
[37] C. Hellriegel, U. Skogsberg, K. Albert, M. Lämmerhofer, N.M. Maier, W. Lindner, J. Am. Chem. Soc. 126 (2004) 3809.

[38] K. Akasaka, K. Gyimesi-Forrás, M. Lämmerhofer, T. Fujita, M. Watanabe, N. Harada, W. Lindner, Chirality 17 (2005) 544.
[39] W. Bicker, I. Chiorescu, V.B. Arion, M. Lämmerhofer, W. Lindner, Tetrahedron: Asymmetry 19 (2008) 97.
[40] H. Dodziuk, W. Kozminski, A. Ejchart, Chirality 16 (2004) 90.
[41] A. Ejchart, W. Kozminski, in: H. Dodziuk (Ed.), Cyclodextrins and Their Complexes, Wiley-VCH, Weinheim, 2006, p. 231.
[42] B. Chankvetadze, G. Endresz, G. Blaschke, Chem. Soc. Rev. 25 (1996) 141.
[43] B. Chankvetadze, G. Blaschke, Electrophoresis 20 (1999) 2592.
[44] H.J. Schneider, F. Hacket, V. Rüdiger, Chem. Rev. 98 (1998) 1755.
[45] G. Sicoli, Z. Jiang, L. Jicsinsky, V. Schurig, Angew. Chem. Int. Ed. 44 (2005) 4092.
[46] G. Sicoli, F. Pertici, Z. Jiang, L. Jicsinszky, V. Schurig, Chirality 19 (2007) 391.
[47] G. Sicoli, I. Tomoyuki, L. Jicsinszky, V. Schurig, Eur. J. Org. Chem. (2008) 4241.
[48] K.B. Lipkowitz, S. Raghothama, J. Yang, J. Am. Chem. Soc. 114 (1992) 1554.
[49] D.W. Armstrong, X. Yang, S.M. Han, R.A. Menges, Anal. Chem. 59 (1987) 2594.
[50] K.B. Lipkowitz, J. Org. Chem. 56 (1991) 6357.
[51] D.W. Armstrong, T.J. Ward, R.D. Armstrong, T.E. Beesley, Science 232 (1986) 1132.
[52] K.B. Lipkowitz, C.M. Stoehr, Chirality 8 (1996) 341.
[53] J. Boger, R.J. Corcoran, J.M. Lehn, Helv. Chim. Acta 61 (1978) 2190.
[54] G. Uccello-Barretta, A. Cuzzola, F. Balzano, R. Menicagli, A. Iuliano, P. Salvadori, J. Org. Chem. 62 (1997) 827.
[55] G. Uccello-Barretta, F. Balzano, A. Cuzzola, R. Menicagli, P. Salvadori, Eur. J. Org. Chem. (2000) 449.
[56] G. Uccello-Barretta, G. Sicoli, F. Balzano, P. Salvadori, Carbohydr. Res. 338 (2003) 1103.
[57] G. Uccello-Barretta, G. Sicoli, F. Balzano, P. Salvadori, Carbohydr. Res. 340 (2005) 271.
[58] J.E.H. Köhler, M. Hohla, M. Richters, W.A. König, Angew. Chem. Int. Ed. Engl. 31 (1992) 319.
[59] G. Uccello-Barretta, A. Cuzzola, F. Balzano, R. Menicagli, P. Salvadori, Eur. J. Org. Chem. (1998) 2009.
[60] G. Uccello-Barretta, L. Ferri, F. Balzano, P. Salvadori, Eur. J. Org. Chem. (2003) 1741.
[61] G. Uccello-Barretta, F. Balzano, G. Sicoli, A. Scarselli, P. Salvadori, Eur. J. Org. Chem. (2005) 5349.
[62] A. Mele, G. Raffaini, F. Ganazzoli, M. Juza, V. Schurig, Carbohydr. Res. 338 (2003) 625.
[63] G. Uccello-Barretta, F. Balzano, A.M. Caporusso, A. Iodice, P. Salvadori, J. Org. Chem. 60 (1995) 2227.
[64] G. Uccello-Barretta, F. Balzano, A.M. Caporusso, P. Salvadori, J. Org. Chem. 59 (1994) 836.
[65] B. Chankvetadze, N. Burjanadze, D.M. Maynard, K. Bergander, D. Bergenthal, G. Blaschke, Electrophoresis 23 (2002) 3027.
[66] D.W. Armstrong, A.M. Stalcup, M.L. Hilton, J.D. Duncan, J.R. Faulkner Jr., S.-C. Chang, Anal. Chem. 62 (1990) 1610.
[67] G. Uccello-Barretta, G. Sicoli, F. Balzano, V. Schurig, P. Salvadori, Tetrahedron: Asymmetry 17 (2006) 2504.
[68] A. Bogdanski, K.L. Larsen, R. Wimmer, Tetrahedron 64 (2008) 1257.
[69] G. Uccello-Barretta, F. Balzano, F. Pertici, L. Jicsinszky, G. Sicoli, V. Schurig, Eur. J. Org. Chem. (2008) 1855.
[70] B. Chankvetadze, G. Pintore, N. Burjanadze, D. Bergenthal, K. Bergander, J. Breitkreuz, C. Mühlenbrock, G. Blaschke, J. Chromatogr. A 875 (2000) 455.
[71] P. Salvadori, G. Uccello-Barretta, F. Balzano, C. Bertucci, C. Chiavacci, Chirality 8 (1996) 423.
[72] K. Uekama, F. Hirayama, T. Imai, M. Otagiri, K. Harata, Chem. Pharm. Bull. 31 (1983) 3363.
[73] E. Yashima, C. Yamamoto, Y. Okamoto, J. Am. Chem. Soc. 118 (1996) 4036.
[74] Y. Okamoto, E. Yashima, Angew. Chem. Int. Ed. 37 (1998) 1020.
[75] T. Kubota, C. Yamamoto, Y. Okamoto, J. Am. Chem. Soc. 122 (2000) 4056.
[76] E. Yashima, J. Chromatogr. A 906 (2001) 105.
[77] T. Kubota, C. Yamamoto, Y. Okamoto, Chirality 14 (2002) 372.
[78] T. Ikai, Y. Okamoto, Chem. Rev., doi:10.1021\cr8005558.
[79] P. Zugenmaier, U. Vogt, Makromol. Chem. 184 (1983) 1749.
[80] U. Vogt, P. Zugenmaier, Ber. Bunsenges. Phys. Chem. 89 (1985) 1217.
[81] C. Yamamoto, E. Yashima, Y. Okamoto, J. Am. Chem. Soc. 124 (2002) 12583.
[82] C.M. Buchanan, J.A. Hyatt, D.W. Lowman, J. Am. Chem. Soc. 111 (1989) 7312.
[83] C.M. Hebling, L.E. Thompson, K.W. Eckenroad, G.A. Manley, R.A. Fry, K.T. Mueller, T.G. Strein, D. Rovnyak, Langmuir 24 (2008) 13866.
[84] K.F. Morris, B.A. Becker, B.C. Valle, I.M. Warner, C.K. Larive, J. Phys. Chem. B 110 (2006) 17359.
[85] B.C. Valle, K.F. Morris, K.A. Fletcher, V. Fernand, D.M. Sword, S. Eldridge, C.K. Larive, I.M. Warner, Langmuir 23 (2007) 425.
[86] S.K. Wiedmer, M.-L. Riekkola, M. Nydén, O. Söderman, Anal. Chem. 69 (1997) 1577.
[87] J.T. Smith, W. Nashabeh, Z.E. Rassi, Anal. Chem. 66 (1994) 1119.
[88] J.K. Rugutt, E. Billiot, I.M. Warner, Langmuir 16 (2000) 3022.
[89] R. Deubner, U. Holzgrabe, J. Pharm. Biomed. Anal. 35 (2004) 459.
[90] K.W. Eckenroad, L.E. Thompson, T.G. Strein, D. Rovnyak, Magn. Reson. Chem. 45 (2007) 72.
[91] J. Tarus, S.A. Shamsi, K. Morris, R.A. Agbaria, I.M. Warner, Langmuir 19 (2003) 7173.
[92] J. Tarus, T. Jernigan, K. Morris, I.M. Warner, Electrophoresis 25 (2004) 2720.
[93] K.F. Morris, A.L. Froberg, B.A. Becker, V.K. Almeida, J. Tarus, C.K. Larive, Anal. Chem. 77 (2005) 254A.
[94] A. Katz, M.E. Davis, Macromolecules 32 (1999) 4113.
[95] M. Yoshida, K. Uezu, M. Goto, S. Furusaki, J. Appl. Pol. Sci. 78 (2000) 695.
[96] M. Yoshida, Y. Hatate, K. Uezu, M. Goto, S. Furusaki, Colloids Surf. A 169 (2000) 259.
[97] L. Malosse, P. Palmas, P. Buvat, D. Adès, A. Siove, Macromolecules 41 (2008) 7834.
[98] H.-W. Sun, F.-X. Qiao, J. Chromatogr. A 1212 (2008) 1.
[99] R.J. Ansell, D. Wang, Analyst 134 (2009) 564.
[100] L. Malosse, P. Buvat, D. Adès, A. Siove, Analyst 133 (2008) 588.
[101] A. Beltran-Porter, D. Beltran-Porter, A. Cervilla, J.A. Ramirez, Talanta 30 (1983) 124.
[102] Y. Lu, C. Li, H. Zhang, X. Liu, Anal. Chim. Acta 489 (2003) 33.
[103] B. Chankvetadze, J. Chromatogr. A 792 (1997) 269.
[104] K. Lomsadze, A.B. Martínez-Girón, M. Castro-Puyana, L. Chankvetadze, A.L. Crego, A. Salgado, M.L. Marina, B. Chankvetadze, Electrophoresis 30 (2009) 2803.